Inviscid flow separation at the crest of an erodible dune

F. Charru[1] and P. Luchini[2]
[1]*Institut de Mécanique des Fluides de Toulouse, CNRS–Université de Toulouse, 31400 Toulouse, France*
[2]*Dipartimento di Ingegneria Industriale, Università di Salerno, 84084 Fisciano, Italy*

The question of the place where a fluid flow separates on a curved obstacle is among the most difficult in fluid mechanics. A criterion based on the cancellation, at that place, of the inviscid flow singularity was proposed by Brillouin [Annal. Chimie Phys. **23**, 145 (1911)] and Villat [J. Math. Pures Appl. **10**, 231 (1914)], which is at the starting point of the triple-deck theory. A similar question arises for the flow over an erodible sand dune with sharp crest, where the *a priori* unknown dune profile and location of the crest result from the coupling of the fluid flow with the sand motion at the dune surface. We show, by computing the potential flow with Levi-Civita's conformal transformation and using a standard closure law for the shear stress driving the sand flux, that the Brillouin-Villat condition here provides the appropriate criterion. We emphasize that within the present model where the bed shear stress is in phase with the flow velocity, so that the flat bed is linearly stable, it is the separation which allows the existence of a self-preserving dune shape. For a dune traveling without deformation on a nonerodible ground, the Brillouin-Villat condition eventually selects its velocity. A parallel is drawn with the Kutta-Joukovski condition for the flow around an airfoil.

DOI: 10.1103/PhysRevFluids.4.034304

I. INTRODUCTION

Sand ripples and dunes are commonly observed patterns, in the natural environment as well as in industry, which result from the interaction of an erodible ground with a liquid or gas flow, see Kennedy [1] for early analyses and Charru *et al.* [2] for a recent review. The formation of such bed forms is usually understood as the result of a linear instability mechanism, where the competition of destabilizing fluid inertia, stabilizing gravity, and particle relaxation phenomena leads to the emergence of some most amplified bed disturbance. Accordingly, the predicted most amplified eigenmode is necessarily sinusoidal in space.

However, observations of sinusoidal bed forms are scarce, even at early stages of their growth, and seem to require carefully prepared loose beds [3]. Most experiments exhibit the development of sawtoothlike patterns (see Refs. [4,5]), as described and analyzed by Bagnold [6]. These bed features grow from randomly distributed small protuberances with size of a few grains and very soon exhibit a sharp rim. This rim most likely causes, and may be caused by, separation of the fluid stream.

Similar observations have been reported for ripples under oscillating flow, such as those created by surface waves. In most conditions, the rolling of individual grains on the flat bed leads to the formation of small ridges with triangular cross sections and spacing much larger than their size [7,8]. Aeolian ripples, on the other hand, although they arise from a quite different mechanism involving saltating grains, also display early coarsening, associated with flow separation and the development of sharp edges [9].

Flow separation over dunes thus appears as a major feature whose importance in the selection of the dune shape and size has as yet received little attention. When identified, the problem is

solved through heuristic arguments, e.g., by assuming that the results of the linearized problem (originally implying attached flow) may still be used, with the dune or hill profile "cut" at some arbitrarily chosen point, beyond which a "separation bubble" takes place [10,11]. The triple-deck theory provides a rational frame for the flow separation problem, as discussed in, e.g., Ref. [12], and in the context of sand dunes in Ref. [13]. As shown in the present paper, inviscid flow calculations together with a condition of regularity at the brink also provide a rational answer to the problem.

Flow separation past an obstacle is a partially open topic in itself, which arises from a complex interaction between a (possibly turbulent) boundary layer and the outer potential flow. Historically, flow separation was first considered by Helmholtz and Kirchhoff, in the context of potential flow, in order to solve the d'Alembert paradox (Ref. [14], Sec. 6.13). Within the "surface-of-discontinuity theory" they developed, the free streamlines issued from the separation points enclose a "wake" of dead fluid with uniform pressure; and along these streamlines, the velocity modulus must then be constant according to Bernoulli's law. A practical conformal-mapping transformation to calculate the Kirchhoff-Helmholtz wake past rounded obstacles was found by Levi-Civita [15]. However, the Kirchhoff-Helmholtz condition does not provide the position of the separation point and, from a strictly mathematical viewpoint, a free streamline can be calculated starting at any chosen point. Whereas for a solid surface with a corner it came natural (what later became the Kutta-Joukovsky condition) to attach the separation streamline at the corner itself, over a smooth surface the position of separation remained undetermined.

It was later observed by Brillouin [16] and Villat [17] that there is in fact a distinguished position (which is today known as the Brillouin-Villat point) where the free streamline is smoother than elsewhere. As will be seen in greater detail in the next section, the slope of the inviscid free streamline generally behaves like a square root near the separation point (so that its derivative, the curvature, is infinite as the power $-1/2$). On considering different candidate separation positions over a given smooth solid surface, regions will be seen where the coefficient of this singular term is negative, so the free streamline goes inside the body and is physically not realizable, and regions where it is positive, where the free streamline is realizable but accompanied by a locally infinite pressure gradient. At the boundary between such regions—the Brillouin-Villat point—the singular term vanishes and curvature and pressure gradient remain finite.

The inviscid theory of separation fails in several respects (in particular, the Kirchhoff-Helmholtz wake expands indefinitely behind the body because of the lack of dissipation), and later in history the emphasis shifted on the boundary layer and its reaction to adverse pressure gradient. However it should be noted that the triple-deck theory of separated flows (e.g., Ref. [12]) represents the position of separation as an asymptotic expansion about the Brillouin-Villat point; in addition, the most compelling objection to all these theories, that they all assume steady flow whereas the practically observed point of separation often moves over a wide span, applies much less to an obstacle protruding from a plane wall, such as a dune, than to a body suspended in free space, because the geometrical obstacle offered by the plane wall greatly restricts the wake oscillations.

In the current dune problem, a corner is present but, owing to the fact that the erodible dune profile couples with the flow and is *a priori* unknown, the position of the corner is unknown too. An indetermination therefore exists, which is similar to that of the position of the separation point on a rounded fixed obstacle. The main purpose of this paper is to show that the Brillouin-Villat criterion may be adopted in order to close the problem and produce a self-maintaining sharp-edged dune shape. It must also be remarked that the separation region behind the avalanche region of a dune is much wider (has a finite angle) than the thin slice (of infinitesimal angle) that initially separates the free streamline from a smooth surface, and therefore boundary-layer interactions are likely to be less influential.

The paper is organized as follows. Section II is devoted to the calculation of the inviscid flow above a rigid obstacle, by the method of conformal transformation, and the application of the Brillouin-Villat condition to the selection of the separation point. A closed-form expression for the position of the Brillouin-Villat point is also provided for the linearized flow. Section III then considers the more complex situation of an erodible dune whose shape results from the

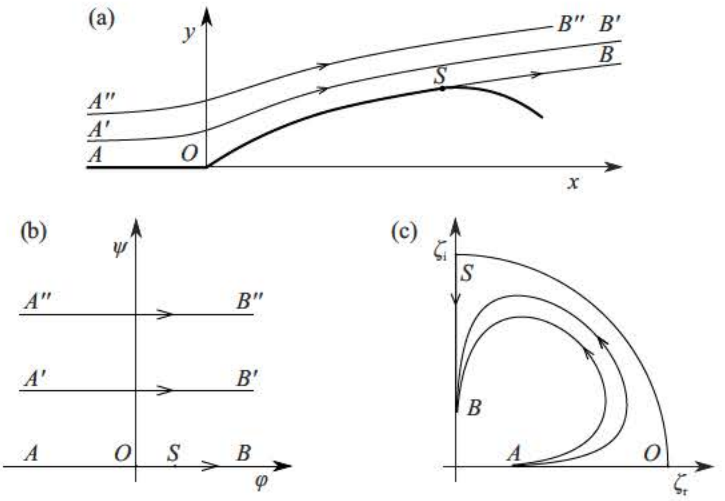

FIG. 1. (a) Potential flow over an obstacle on a flat ground, with separation point S, (b) corresponding points and streamlines in the F plane, and (c) in the Levi-Civita ζ plane.

interaction of the fluid flow with the thin sand layer moving at the dune surface. Emphasis is put on dunes traveling without deformation on a nonerodible ground, where the Brillouin-Villat condition provides the dune velocity. The final section, IV, discusses the results and their relevance with regard to experiments.

II. FLOW OVER A FIXED OBSTACLE

A. Base problem

Let us consider a two-dimensional obstacle over a flat ground, as that shown in Fig. 1(a), with profile

$$H(x, y) = y - h(x) = 0, \quad \text{for } x > 0. \tag{1}$$

The fluid flows from left to right with undisturbed velocity U at infinity and separates from the obstacle at some point S, with abscissa x_s. The separation point may physically correspond to a small protrusion or a sharp edge. The free streamline originating from S divides the fluid region in two parts: the flowing region above, where the velocity potential ϕ satisfies the Laplace equation

$$\Delta\phi = 0, \tag{2}$$

and a "Helmholtz wake" below, of quiescent fluid with uniform pressure equal to its value at infinity. For the purpose of nondimensionalization, the velocity U at infinity is taken as the reference velocity and a characteristic dimension of the obstacle, say L, as the reference length.

The boundary conditions associated with the Laplace equation are, first, that far from the obstacle, the fluid velocity must match with the undisturbed velocity $U = 1$. Second, on the lower boundary $AOSB$ corresponding to the streamline $\psi = 0$, the velocity components u and v must satisfy the following conditions:

$$v = 0 \quad \text{on the flat wall } AO, \tag{3a}$$

$$v/u = \partial_x h \quad \text{on the obstacle } OS, \tag{3b}$$

$$u^2 + v^2 = 1 \quad \text{on the free streamline } SB. \tag{3c}$$

The solution of the above problems (2) and (3), for a given obstacle and a given position x_s of the separation point, can be searched by the method of conformal transformation. In the complex plane $z = x + iy$, the complex fluid velocity $w = u - iv$ is related to the complex potential $F = \phi + i\psi$ by

$$w = \frac{dF}{dz}, \quad w = u - iv = |w| \exp(-i\theta), \tag{4}$$

with the foot O of the obstacle corresponding to $z = w = F = 0$.

Following the method introduced by Kirchhoff and Helmholtz (Ref. [14], Sec. 6.13), let us introduce the new complex variable

$$\omega = -\log w = -\log |w| + i\theta, \tag{5}$$

for which the boundary conditions (3) become

$$\omega_\mathrm{i} = 0 \quad \text{along} \quad AO, \tag{6a}$$

$$\omega_\mathrm{i} = \arctan(\partial_x h) \quad \text{along} \quad OS, \tag{6b}$$

$$\omega_\mathrm{r} = 0 \quad \text{along} \quad SB. \tag{6c}$$

where ω_r and ω_i are the real and imaginary parts of ω. For a polygonal obstacle with straight faces, the lower boundary of the flow domain is therefore represented in the ω plane by a straight-sided figure, and the problem of the correspondence between the z plane and the F plane can be solved using the Schwarz-Christoffel theorem. For a curved obstacle such as that shown in Fig. 1(a), the solution was found by Levi-Civita (1907) with the help of the conformal transformation

$$F = -\frac{\phi_s}{4}\left(\zeta - \frac{1}{\zeta}\right)^2, \quad \zeta = \sqrt{1 - F/\phi_s} - \sqrt{F/\phi_s}, \tag{7}$$

which maps the upper-half F plane [Fig. 1(b)] inside the quarter circle ζ [Fig. 1(c)]. Along the streamline $\psi = 0$, in particular, the flat ground AO corresponds to real ζ with $\zeta_\mathrm{r} \leqslant 1$, the obstacle OS corresponds to $\zeta = \mathrm{e}^{\mathrm{i}\beta}$ with argument β increasing from zero to $\pi/2$, and the free streamline SB, to imaginary ζ with $\zeta_\mathrm{i} \leqslant 1$. The parameter ϕ_s, *a priori* unknown, corresponds to the value of the potential at the separation point, where $\zeta = i$. Then consider the expansion

$$\omega = -\log |w| + i\theta = a_1\zeta + a_3\zeta^3 + a_5\zeta^5 + \cdots \tag{8}$$

with real coefficients a_j. Such an expansion ensures that the boundary conditions (6a) and (6c) are automatically satisfied: ζ real along the ground AO satisfies $v = 0$, and ζ and its odd powers imaginary along the free streamline SB satisfy $|w| = 1$. Then, the coefficients a_j appear as the coefficients of the Fourier series in $\sin(2n+1)\beta$, with $n = 0, 1, 2, \ldots$, of the local angle $\theta = \tan^{-1} \partial_x h$ of the obstacle.

Thus, for any set of coefficients a_j, representing some specific profile $H(x, y) = 0$, Eqs. (7) and (8) provide a parametric relationship between F and w which satisfies all the boundary conditions. Integration of (4) along the streamline $AOSB$ ($\psi = 0$),

$$z - z_A = \int_{F_A}^{F} \frac{dF}{w}, \tag{9}$$

or along any streamline $A'B'$, then solves the problem, with the separation point at the place where $F = \phi_s$ (and $\zeta = i$). In the above equation, the position z_A of the far upstream starting point A, with complex potential F_A (with $\phi_A \ll 0$), can be obtained from the approximate solution

$$z_A \sim F_A - \frac{2\alpha}{\pi}(-F_A)^{1/2},$$

where $\alpha = \tan^{-1} h'(0)$ is the slope angle at the foot O of the obstacle.

A difficulty with the Levi-Civita transformation is that the function $\omega(\zeta)$ (8) corresponding to a given $H(x, y) = 0$ is *a priori* unknown, so that the determination of the coefficients a_j is part of the problem. This difficulty was first overcome by Villat, who provided the correspondence under the form of an integrodifferential equation. Here, however, an iterative Newton's method will be used rather than Villat's method, starting with a set of guess coefficients a_j and computing their variations until (1) is satisfied. This method can indeed be adapted to the more general problem addressed in the next section.

Note that the flow exhibits a singularity at the stagnation point O (infinite velocity gradient and pressure gradient), so that a large number of terms in the expansion (8) may be required for convergence to be achieved. This number can be greatly reduced by accounting for the singularity with the supplementary logarithmic term

$$a_0 \log \frac{1-\zeta}{1+\zeta} \quad \text{with } a_0 = -\frac{2\alpha}{\pi}. \tag{10}$$

This term provides in fact the solution for the flow over a triangular obstacle with inclination α to the ground, with all other coefficients in Eq. (8) equal to zero (the corresponding flow being that around a corner with angle $\pi - \alpha$; see, e.g., Ref. [14], Sec. 6.5).

B. Separation point imposed

We now consider the situation where flow separation is provoked, by a sharp edge or some small protrusion, at some imposed point S of the profile of the obstacle, with abscissa x_s.

Let $a_j^{(0)}$, $j = 1 \ldots N$, and $\phi_s^{(0)}$ be a set of $N + 1$ starting coefficients, associated through Eqs. (7)–(9) to some profile

$$H^{(0)} = y^{(0)} - h\big(x^{(0)} - x_0^{(0)}\big), \tag{11}$$

where $x_0^{(0)}$ is the computed abscissa of the foot O. This profile does not satisfy *a priori* Eq. (1) of the obstacle (i.e., $H^{(0)} \neq 0$) or the desired location of the separation point (i.e., $x_s^{(0)} = x(\phi_s^{(0)}) \neq x_s$). Corrections δa_j and $\delta\phi_s$ need therefore to be determined. Differentiating (1), these corrections must satisfy, at first order,

$$\delta y - (\delta x - \delta x_0)\partial_x h^{(0)} = -H^{(0)}, \tag{12}$$

where $\partial_x h^{(0)} = \partial_x h(x^{(0)} - x_0^{(0)})$ is the slope at the point with abscissa $x^{(0)} - x_0^{(0)}$, and δx and δy are related to the δa_j through the relation

$$\delta x + i\delta y = \delta\phi_s \int_{F_A}^{F} \frac{d(F/\phi_s)}{w^{(0)}} + \delta a_1 \phi_s \int_{F_A}^{F} \zeta \, \frac{d(F/\phi_s)}{w^{(0)}} + \delta a_3 \phi_s \int_{F_A}^{F} \zeta^3 \, \frac{d(F/\phi_s)}{w^{(0)}} + \cdots . \tag{13}$$

Imposing that (12) with δx and δy given by (13) be satisfied at N collocation points along the profile OS provides N linear equations for $N + 1$ unknowns. (A convenient discretization corresponds to equally spaced ζ_k ($k = 1 \ldots N$) along the quarter-circle OS.) The last equation is provided by the condition that the separation point be at the desired location:

$$\delta x = -\big(x_s - x_s^{(0)}\big) \quad \text{at } \zeta = i. \tag{14}$$

Inversion of the system (12)–(14) provides $\delta\phi_s$ and the N corrections δa_j, and thus new coefficients $V^{(1)} = V^{(0)} + \delta V$ and $a_j^{(1)} = a_j^{(0)} + \delta a_j$, $j = 1 \ldots N$. Iterating until convergence provides the solution for ϕ_s and the a_j. A fine representation of the overall flow is achieved with a small number of coefficients, typically less than ten. However, more coefficients are required for a thorough representation of the flow in the vicinity of the separation point where a singularity generally remains, as shown below.

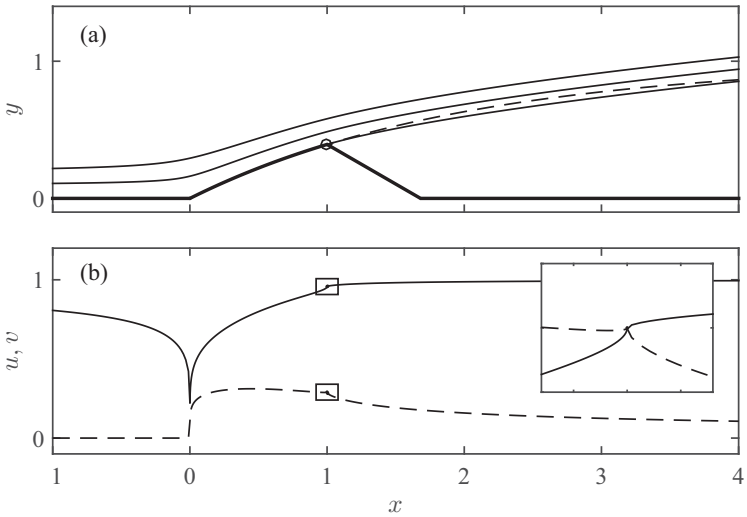

FIG. 2. (a) Flow above the exponential obstacle (15) with $\ell = 2$ and $x_s = 1$ imposed ($\phi_s = 0.882$, $a_0 = -2/\pi \tan^{-1}(1/\ell) = -0.295$, $a_1 = -0.155$, and $a_3 = 0.0184$); dashed line: virtual profile (15) beyond the separation point; (b) velocities u (−) and v (- -) along the streamline $\psi = 0$; inset: enlargement of the small rectangles around the points (x_s, u_s) and (x_s, v_s).

As an illustration, consider an exponential obstacle ending with a sharp brink at $x = x_s$, represented by the equation

$$h(x) = 1 - \exp(-x/\ell) \quad \text{for } 0 < x < x_s. \tag{15}$$

Figure 2(a) displays computed streamlines for $\ell = 2$ and $x_s = 1$. The corresponding values of ϕ_s and the two first coefficients a_1 and a_3 are given in the caption. It can be noted that the free streamline passes a little below the exponential profile being prolonged beyond the separation point (dashed line). For larger x_s (say $x_s = 3$, not shown), the free streamline lies slightly above the prolonged obstacle. The latter situation may also correspond to separation not at a sharp edge, but at a regular point of a smooth profile.

Figure 2(b) displays the velocity components u and v along the streamline $\psi = 0$. The velocity vanishes at the stagnation point O, as expected, then increases along the obstacle up to some maximum in between O and S, and decreases again. The inset focuses on the behavior of the velocity components in the small rectangles around the points (x_s, u_s) and (x_s, v_s) where the complex velocity is

$$w_s = u_s - iv_s = e^{-i\theta_s}, \quad \theta_s = -\frac{\pi}{2}a_0 + a_1 - a_3 + a_5 - \cdots. \tag{16}$$

It can be seen that both components display singular behavior at the separation point, which is associated with the divergence of the curvature of the free streamline there.

C. Brillouin-Villat condition imposed

The existence of a sharp edge on the profile of an obstacle promotes flow separation at this point. However, as shown above, the fluid velocity generally exhibits a singularity there. The question then arises whether some design of the obstacle might eliminate this singularity. On the other hand, on a smooth profile, there exists an infinite number of possible positions of the separation point [each corresponding to some function $\omega(\zeta)$ (8)]. The question here is the existence of a particular point where separation would most likely occur. The Brillouin-Villat condition provides the desired answer to these two questions.

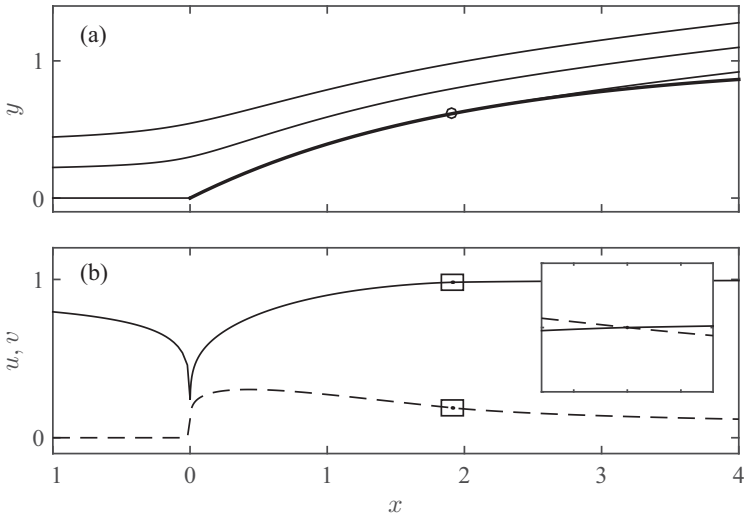

FIG. 3. (a) Streamlines and (b) u and v along the streamline $\psi = 0$ for the same exponential profile as in Fig. 2, now unbounded. The Brillouin-Villat condition $B = 0$ gives $x_s = 1.91$; inset: enlargement around the points (x_s, u_s) and (x_s, v_s), showing that the singularity has disappeared ($\phi_s = 1.78$, $a_1 = -0.257$, and $a_3 = -0.0239$).

Let us consider the velocity singularity more closely and expand (8) in the neighborhood of $\zeta = i$ (the separation point). We find

$$-\log w \sim -\log w_s + B\,(\zeta - i),$$

where w_s is defined by (16) and B by

$$B = \frac{d\omega}{d\zeta}(\zeta = i) = -a_0 + a_1 - 3a_3 + 5a_5 - \cdots . \tag{17}$$

Then, from (7) and (4),

$$\zeta - i \sim \pm\frac{i}{2}\left(\frac{F - F_s}{\phi_s}\right)^{1/2} \sim \pm\frac{i}{2}\left(\frac{w_s(z - z_s)}{\phi_s}\right)^{1/2},$$

where the sign $+$ (resp. $-$) holds upstream (resp. downstream) of point S. We finally obtain the velocity as

$$\frac{w}{w_s} \sim 1 \mp \frac{iB}{2}\left(\frac{w_s}{\phi_s}\right)^{1/2}(z - z_s)^{1/2}. \tag{18}$$

This expression agrees with the square-root behavior displayed in the inset of Fig. 2(b).

As first noticed by Brillouin (1911) and Villat (1914), the singularity disappears if the coefficient of $(z - z_s)^{1/2}$ cancels, that is, for $B = 0$. This condition may be satisfied for some particular set of coefficients a_j and corresponding x_s, which can be searched for through a slight modification of the linear system (12)–(14): It suffices to replace Eq. (14), which imposes the separating point at some location x_s, by the linearization of the equation $B = 0$ in the neighborhood of the previous iteration:

$$\delta a_1 - 3\delta a_3 + 5\delta a_5 - \cdots = -\big(-a_0 + a_1^{(0)} - 3a_3^{(0)} + 5a_5^{(0)} - \cdots\big). \tag{19}$$

Figure 3(a) displays, for the same exponential profile as in Fig. 2(a), the new solution satisfying (19): The computed separation point is now located at $x_s = 1.91$ (where $\phi_s = 1.78$). Figure 3(b) displays the velocity components u and v along the streamline $\psi = 0$, while the enlargement in

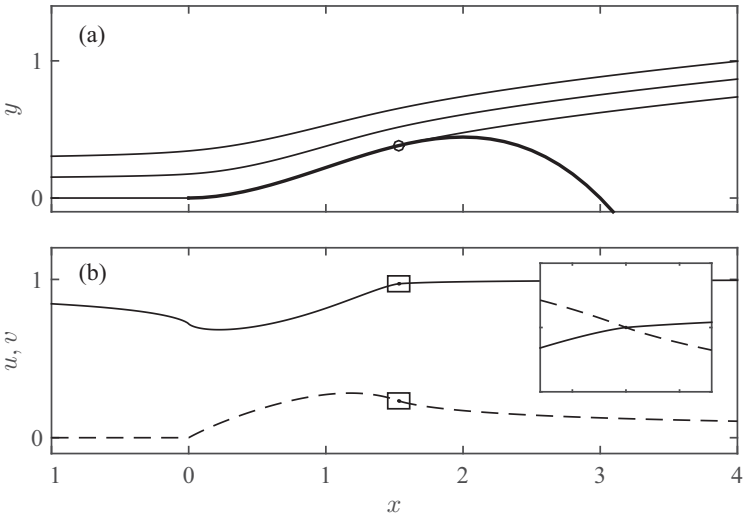

FIG. 4. (a) Streamlines over the smooth polynomial obstacle $h/\ell = (x/\ell)^2 - (x/\ell)^3$ with $\ell = 3$: The Brillouin-Villat condition gives $x_s = 1.53$; (b) velocity components u and v; inset: enlargement around the points (x_s, u_s) and (x_s, v_s) ($\phi_s = 1.29$, $a_0 = 0$, $a_1 = 0.332$, and $a_3 = 0.0688$).

the inset confirms that the singularity has been removed. Note that, unlike in Fig. 2(a), the free streamline now lies everywhere above the exponential curve.

Another illustration, for a polynomial profile, is shown in Fig. 4. The Brillouin-Villat condition here gives the location of the separation point at $x_s = 1.53$. Note that the slope is now continuous at the foot ($x = 0$), so that the velocity no longer vanishes. However, a singularity remains there, associated with a divergence of the curvature of the velocity profile.

Finally, the Brillouin-Villat condition may be interpreted in two ways, depending on the geometry of the obstacle: Over a smooth profile, it defines a unique separation point; over a sharp-edged profile, it provides a distinguished size of the obstacle and location of the sharp edge, with both situations corresponding to regular flow there.

D. Brillouin-Villat condition for linearized flow

In the approximation of small slope $\partial_x h$ of the obstacle, the fluid flow can be described by linearized potential theory, also known in aerodynamics as thin airfoil theory (Ref. [14], Sec. 6.9). At leading order, this flow is unperturbed by the modulation of the bottom and is just characterized by the uniform velocity $U = 1$.

At the next order of approximation, the complex velocity is $1 + \widetilde{w}$, where $\widetilde{w} = \widetilde{u} - i\widetilde{v}$ is a small perturbation induced by the bottom. Hilbert's formula allows the complex velocity $\widetilde{w}$ in the upper half-plane $y > 0$ to be calculated from its imaginary part on $y = 0$ as

$$\widetilde{w}(z) = \frac{1}{\pi} \int_{-\infty}^{\infty} \frac{\widetilde{v}(\xi)}{z - \xi} d\xi . \tag{20}$$

The boundary conditions are

$$\begin{aligned} &\widetilde{v} = 0 \quad \text{for} \quad x < 0, \\ &\widetilde{v} = h' \equiv \partial_x h \quad \text{for} \quad 0 < x < x_s, \\ &\widetilde{u} = 0 \quad \text{for} \quad x > x_s, \end{aligned}$$

the latter deriving from $1 = U^2 = (1 + \widetilde{u})^2 + \widetilde{v}^2 \simeq 1 + 2\widetilde{u}$.

To determine a complex analytic function obeying such mixed boundary conditions constitutes what is known as a Riemann-Hilbert problem and, just like in thin-airfoil theory, it can be solved by applying (20) to the analytic function $\widetilde{w}(z)/(x_s - z)^{1/2}$ in the place of $\widetilde{w}$. The result is

$$\widetilde{w}(z) = \frac{(x_s - z)^{1/2}}{\pi} \int_0^{x_s} \frac{h'(\xi)}{(x_s - \xi)^{1/2}(z - \xi)} d\xi, \tag{21}$$

where the integration interval can be restricted to $[0, x_s]$ because the imaginary part of $\widetilde{w}(x)/(x_s - x)^{1/2}$ is zero for $x < 0$ (where it is proportional to $\widetilde{v}$) and for $x > x_s$ (where it is proportional to $\widetilde{u}$).

In order to determine the velocity in a neighborhood of the separation point, we cannot just set $z = x_s$ in Eq. (21) because the integral would not converge. Instead, we add and subtract $h'(x_s)$ to the numerator under the integral to obtain

$$\widetilde{w}(z) = \frac{(x_s - z)^{1/2}}{\pi} \left[\int_{-\infty}^{x_s} \frac{h'(\xi) - h'(x_s)}{(x_s - \xi)^{1/2}(z - \xi)} d\xi + \int_{-\infty}^{x_s} \frac{h'(x_s)}{(x_s - \xi)^{1/2}(z - \xi)} d\xi \right].$$

Now the first integral is convergent for $z \to x_s$, and we may directly set $z = x_s$ in it, whereas the second can be integrated analytically. We then obtain the required local power expansion as

$$\widetilde{w}(z) = -ih'(x_s) + c_{BV}(x_s - z)^{1/2} + O(x_s - z) \tag{22}$$

with

$$c_{BV} = \frac{1}{\pi} \int_{-\infty}^{x_s} \frac{h'(\xi) - h'(x_s)}{(x_s - \xi)^{3/2}} d\xi = -\frac{2}{\pi} \int_{0^-}^{x_s} \frac{h''(\xi)}{(x_s - \xi)^{1/2}} d\xi, \tag{23}$$

the second form having been obtained through integration by parts. Care should be taken, if the second expression of c_{BV} is adopted for a wall profile that discontinuously acquires a nonzero slope at $x = 0$, to include a suitable δ function in h'' representing this kink. The lower bound of the integral has been denoted as 0^- to indicate this.

The constant term of (22) is nothing else than the imposed boundary condition on velocity, the $\widetilde{v}$ component of which must equal $h'(x_s)$. The second term represents the deviation from this value; consequently the slope of the free streamline, after separation where $(x_s - z)^{1/2}$ is negative imaginary, is greater or smaller than its value before separation according to the sign of c_{BV}. In addition, its derivative (the curvature of the free streamline) is infinite for all $c_{BV} \neq 0$. Similarly, before the point of separation, where $(x_s - z)^{1/2}$ is real, the $\widetilde{u}$ component has the same sign as c_{BV} while its derivative for $c_{BV} \neq 0$ is infinite, and so is the pressure gradient.

The special value (or values) of x_s such that $c_{BV} = 0$ guarantees that curvature and pressure gradient remain continuous. This is the Brillouin-Villat condition $B = 0$ already discussed, see Eq. (17), of which (23) provides the linearized version. The integral that appears in Eq. (23) is sometimes named the fractional derivative of order $-1/2$ of h'', or the fractional derivative of order $3/2$ of h. Therefore, the Brillouin-Villat condition for linearized flow can be compactly stated as "separation occurs at the point where the $3/2$ derivative of surface height crosses zero."

As an illustration, let us compute, for the exponential profile (15), the position x_s of the edge, i.e., the separation point, satisfying the Brillouin-Villat condition (23). Inserting (15) into (23) gives

$$\frac{\pi}{2} c_{BV} = -\frac{1}{\ell x_s^{1/2}} + \int_0^{x_s} \frac{\exp(-x/\ell)}{\ell^2 (x_s - x)^{1/2}} dx = 0.$$

The above integral belongs to the family of the error function (it can be reduced to Dawson's integral) and can easily be evaluated numerically to provide the unique solution

$$x_s/\ell \simeq 0.854033. \tag{24}$$

Figure 5 compares this solution with those of the nonlinear problem with increasing foot slope ℓ^{-1}: as expected, the linear solution is recovered in the limit $\ell^{-1} \to 0$.

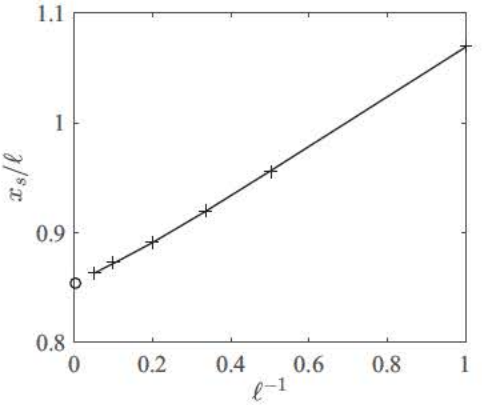

FIG. 5. Position x_s of the separation point on the exponential profile (15) as a function of the slope ℓ^{-1} at the foot O, according to the Brillouin-Villat condition: (+), nonlinear solution ($B = 0$); (○), linear solution (24).

III. ERODIBLE DUNES

The dynamics of erodible sand beds sparked off a large number of studies, aiming at understanding, in particular, the observed instability of a flat bed and the wavelength of the resulting sand ripples, or the dynamics of isolated "barchan dunes" propagating over a nonerodible flat ground; see, e.g., Ref. [2] for a recent review. A striking feature of such bed forms is that, as soon as the fluid velocity exceeds some threshold for sand motion and the bed form grows, the fluid flow immediately separates and an avalanche face develops on the lee side. Such a separation, which likely plays an important role in the selection of the dune size, cannot be addressed within the framework of linearized equations, and few analyses have tackled, in this context, the nonlinear problem. One difficulty is that, contrary to the situation addressed in the previous section, the dune profile is not *a priori* known but is generated out of a complex interaction between the fluid flow and the rheology of the sheared sand layer at the dune surface. However, potential flow analysis together with the Brillouin-Villat condition provides, as shown in this section, a basic answer to the question of the selection of the dune size and profile.

A. Boundary condition on the erodible dune surface

1. Shear stress

In the present framework of inviscid flow, the shear stress τ moving the grains can be related to the local surface velocity $|w|$, as computed from the inviscid analysis, by the empirical formula

$$\tau = \rho u_\tau^2 = c_f \, \tfrac{1}{2} \rho |w|^2 \tag{25}$$

with, for large-Reynolds-number turbulent flow, a constant friction coefficient c_f. The question of whether this relationship, largely used in hydraulic engineering, does or does not correspond to some asymptotic limit (for small wave number or large Reynolds number) accounting for boundary-layer phenomena, is still today probably unanswered. Some more elaborate relationship would be preferable, based on the linear response of the flow over a sinusoidal bed disturbance (i.e., $\tau/\partial_x h$ as a function of the dimensionless wave number $k^+ = kv/u_\tau$). Benjamin [18] and Hunt *et al.* [19] provided such analyses, but some of their hypotheses (laminar flow, or mixing-length turbulence modeling) remain questionable. Luchini and Charru [20] provided an interpolated transfer function in the range $k^+ > 10^{-3}$, in agreement with asymptotic analyses, direct numerical simulations, and experiments. However, no such transfer function is available in the small-wave-number limit where the present inviscid calculations are relevant. Finally, Eq. (25) appears as a reasonable choice for the

present purposes, where the objective is the assessment of the Brillouin-Villat condition as a tool for predicting separation at an erodible sharp edge.

2. Sand transport

For the relationship between the bed shear stress $\tau(|w|, \partial_x h)$ and the particle flux q (volume per unit time and unit transverse length), several choices are available in the literature; see, e.g., Lajeunesse *et al.* [21] for some of them. We choose here the one proposed by Fernandez Luque and van Beck [22]:

$$\frac{q}{V_s d} = a\sqrt{\theta}(\theta - \theta_t), \quad \theta_t = \theta_{t0}(1 + \partial_x h/\mu). \tag{26}$$

In this equation, $V_s = [(\rho_p/\rho - 1)gd]^{1/2}$ is a characteristic settling velocity with d and ρ_p being the diameter and density of the grains, $\theta = \tau/(\rho_p - \rho)gd$ is a dimensionless shear stress (known as the Shields number), θ_{t0} is the threshold for particle motion over a horizontal bed, and θ_t is the corresponding threshold over a bed with local slope $\partial_x h$. Finally, $a \approx 10$ is a constant and μ is a friction coefficient which parametrizes the effect of the gravity component parallel to the slope.

3. The dune equation

The last equation closing the boundary condition problem is the mass conservation for the grains,

$$\partial_t h + \partial_x q = 0. \tag{27}$$

Introducing the dimensionless time T, height H, and space coordinate X as

$$T = a\theta_{t0}^{3/2}\frac{V_s d}{L^2}\,t, \quad H = \frac{h}{L}, \quad X = \frac{x}{L}, \tag{28}$$

where L is an arbitrary length (related to the available volume of sand), Eqs. (25)–(27) provide the final dune equation:

$$\partial_T H + \partial_X Q = 0, \quad \text{with } Q = \frac{|w|}{u_t}\left(\frac{|w|^2}{u_t^2} - 1 - \frac{1}{\mu}\,\partial_X H\right). \tag{29}$$

This nonlinear equation, second order in space and first order in time, couples the fluid flow, through the velocity ratio $|w|/u_t$, with the bed height. It depends on two dimensionless parameters: the threshold fluid velocity u_t and the friction coefficient μ. Since the velocity $|w|$ along the dune appears only through the ratio $|w|/u_t$, the velocity scale can be so chosen that the fluid velocity $U = 1$ at infinity, as in the previous section. The threshold $u_t < 1$ then corresponds to the fraction of velocity at infinity which first moves the sand.

B. Analytical solution of a simplified problem

1. Simplified problem

We first consider the simplified problem where the fluid velocity is assumed to be uniform and equal to unity from the dune foot O up to the separation point S. This assumption is consistent with the fact that, as far as the slope of the obstacle remains small, $|w|$ is close to the undisturbed velocity $U = 1$ all along the dune. The sand transport equation then reduces to

$$Q = Q_0 - Q_1\partial_X H, \quad Q_0 = \frac{1}{u_t}\left(\frac{1}{u_t^2} - 1\right), \quad Q_1 = \frac{1}{u_t\mu}, \tag{30}$$

where Q_0 and Q_1 are constant coefficients. The dune equation (29) then decouples from the fluid flow problem and reduces to the linear diffusion equation

$$\partial_T H + Q_1\partial_{XX} H = 0, \tag{31}$$

with constant and positive Q_1. All its continuous solutions with homogeneous boundary conditions ($H = 0$ far upstream and downstream) decay to a flat surface with time. Nevertheless, flow separation and the development of an avalanche face allows for discontinuous solutions which do not decay, in particular traveling steady solutions.

2. Traveling dune solution

Thus we now search for a traveling dune solution, propagating without deformation over a nonerodible ground with velocity V to be determined. In the reference frame moving with the dune, the dune equation (29) reduces to $-V\partial_X H + \partial_X Q = 0$, which integrates to

$$-VH + Q = 0 \quad \text{with} \quad Q = Q_0 - Q_1 \partial_X H,$$

where the integration constant, which would correspond to some sand flux coming from upstream, must be set to zero for a dune traveling with constant volume. A second integration accounting for the condition $H(0) = 0$ then provides the exponential solution

$$H/H_\infty = 1 - \exp(-X/q_1 H_\infty), \quad H_\infty = \frac{Q_0}{V}, \quad q_1 = \frac{Q_1}{Q_0} \tag{32}$$

(which, not by accident, was chosen as a test profile to illustrate the phenomenon of separation in some of the previous sections).

3. Dune velocity

The determination of the unknown velocity V requires some additional condition related to the finite size of the dune, or, in other words, a condition stating that the profile (32) is "cut" at some point, where the flow separates and an avalanche face develops. The Brillouin-Villat condition provides a distinguished position X_s for this point, where the singular behavior of the fluid velocity cancels. For linearized flow, Eq. (24) provided this position for an exponential profile, which here becomes

$$\frac{X_s}{q_1 H_\infty} \simeq 0.854033. \tag{33}$$

Now consider the volume of the dune (per unit transverse length)

$$A = \int_0^{X_s} H(X) dX + \frac{H_s^2}{\tan(\pi/6)},$$

where the second term accounts for the volume under the avalanche face assumed to have a slope of $\pi/6$. With (32) and (33), this volume becomes

$$A \simeq (0.280\, q_1 + 0.571)\, H_\infty^2.$$

For given A and with $H_\infty = Q_0/V$, the above relationship provides the desired velocity:

$$V \simeq (0.280\, q_1 + 0.571)^{1/2} \frac{Q_0}{A^{1/2}}. \tag{34}$$

This results recovers, in particular, the well-known result that the velocity of a dune is inversely proportional to its characteristic size.

4. Back to dimensional quantities

The most convenient choice for the free length scale L now appears to be the square root of the dimensional volume A_{dim} of the dune, so that the above dimensionless volume $A = A_{\text{dim}}/L^2$ is unity. The dimensional velocity V_{dim} is then given by

$$V_{\text{dim}} \simeq (0.280\, q_1 + 0.571)^{1/2} \frac{Q_{0,\text{dim}}}{A_{\text{dim}}^{1/2}}, \quad \text{with} \quad Q_{0,\text{dim}} = a\theta_{t0}^{3/2} V_s d\, Q_0. \tag{35}$$

The dimensional position and height of the separation point are finally given by

$$X_{s,\mathrm{dim}} \simeq 0.854\, q_1 H_{\infty,\mathrm{dim}}, \tag{36}$$

$$H_{s,\mathrm{dim}} \simeq [1 - \exp(-0.854)]\, H_{\infty,\mathrm{dim}}, \tag{37}$$

with $H_{\infty,\mathrm{dim}} = (0.280\, q_1 + 0.571)^{-1/2} A_{\mathrm{dim}}^{1/2}$.

C. Numerical solution for traveling dunes

We now return to the full problem where the irrotational flow couples with the erodible dune, and search, as before, for traveling dunes propagating without deformation over a nonerodible ground with velocity V. In the reference frame moving with the dune, the mass conservation equation (27) reduces to $-V\partial_X H + \partial_X Q = 0$, which, for zero sand flux from upstream, integrates to $-VH + Q = 0$. The final boundary equation for the flow above the dune becomes

$$\mathcal{L}(H, \partial_X H, |w|/u_t) = 0, \tag{38}$$

where the operator $\mathcal{L}$ is defined by

$$\mathcal{L} = -VH + Q(|w|/u_t, \partial_X H) \tag{39}$$

and Q is given by (29). For the present erodible boundary, this differential equation replaces the slip condition (3b) holding for fixed obstacles.

Solving (38) for a given velocity distribution $|w|/u_t$, requires, in addition to the boundary condition $H(0) = 0$, another condition determining the position of the separation point and the velocity V. The Brillouin-Villat condition, again, provides the required equation.

1. Numerical method

The numerical method follows the same lines as for the fixed obstacle with the new unknown V, and velocity potential at the separation point set to $\phi_s = 1$ in Eq. (7). Starting with guess coefficients $V^{(0)}$ and $a_j^{(0)}$, $j = 1 \ldots N$, the corresponding dune profile $H^{(0)}$ is first computed from Eqs. (7)–(9). The corresponding equation

$$\mathcal{L}^{(0)} = -V^{(0)} H(x^{(0)}) + Q(|w|^{(0)}/u_t, \partial_X H^{(0)})$$

does not *a priori* satisfy $\mathcal{L}^{(0)} = 0$ as required by (38). Corrections δa_j and δV need to be found, which at first order satisfy

$$\delta\mathcal{L} = -\mathcal{L}^{(0)}, \tag{40}$$

where

$$\delta\mathcal{L} = -V^{(0)}\delta H - H(x^{(0)})\delta V + \frac{\partial Q}{\partial |w|}^{(0)} \delta|w| + \frac{\partial Q}{\partial(\partial_X H)}^{(0)} \delta(\partial_X H)$$

and where the variations δV, δH, $\delta(\partial_X H)$, and $\delta|w|$ are linear functions of the δa_j computed from Eqs. (7)–(9) (with $\phi_s = 1$).

Imposing that (40) be satisfied at N collocation points along the dune profile OS gives N linear equations for $N + 1$ unknowns. The last equation is provided by the Brillouin-Villat condition (19). Inversion of this linear system provides δV and the N corrections δa_j and thus new coefficients $a_j^{(1)} = a_j^{(0)} + \delta a_j$ and $V_s^{(1)} = V_s^{(0)} + \delta V_s$. Iterating until convergence gives the solution for V and the a_j.

2. Results

Figure 6(a) displays the dune profile computed from (38) and the Brillouin-Villat condition, for the parameters given in the caption. The fluid velocity [Fig. 6(b)] does not display any singularity

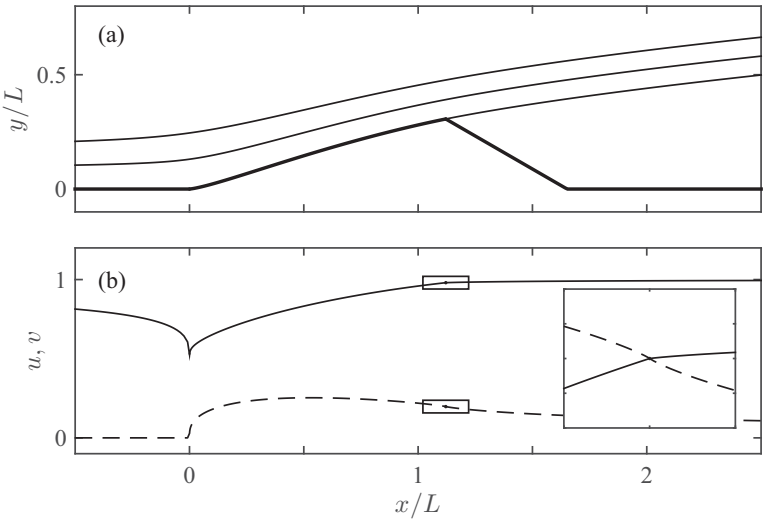

FIG. 6. (a) Streamlines over a traveling erodible dune for the transport law (26); (b) corresponding velocities u and v along the streamline $\psi = 0$; inset: enlargement around the points (x_s, u_s) and (x_s, v_s). The Brillouin-Villat condition selects $x_s = 1.12$ and the dune velocity and volume $V = 17.0$ and $A = 0.259$ ($\mu = 0.5$, $u_t = 0.5$).

at the separation point, as expected. Note that the dune profile has smooth continuous slope at the foot, unlike the exponential dune. The velocity does not vanish there, but still exhibits a singularity associated with a singularity of the curvature of the dune profile.

Decreasing the threshold velocity u_t (i.e., increasing the flow velocity) only slightly changes the position of the separation point (from $x_s = 1.05$ for $u_t = 0.8$ to $x_s = 1.13$ for $u_t = 0.2$), and increases the dimensionless volume (from $A = 0.0604$ for $u_t = 0.8$ to $A = 0.608$ for $u_t = 0.2$), giving stockier profiles with larger slopes and larger velocity. Varying the friction coefficient μ has a weak effect (an increase from 0.2 to 0.8 changes x_s by 4% and increases the volume by a factor of about 2, while the dune velocity V decreases from 20.9 to 16.0).

The sensitivity of the previous results to the sand transport equation can now be assessed. Since the fluid velocity along the dune does not vary much, one may first consider the law (26) previously used, linearized about $|w| = 1$ and small slope $\partial_X H$, that is

$$Q = Q_0 - Q_1 \partial_X H + Q_2(|w| - 1) \tag{41}$$

with positive coefficients

$$Q_0 = \frac{1}{u_t}\left(\frac{1}{u_t^2} - 1\right), \quad Q_1 = \frac{1}{u_t \mu}, \quad Q_2 = \frac{1}{u_t}\left(\frac{3}{u_t^2} - 1\right).$$

Figure 7 displays the corresponding streamlines and velocity profiles. The dune foot here appears flatter, which can be understood by the fact that the linearization overestimates the flow velocity there, with resulting flattened overall profile.

The third sand transport law that we consider is the widely used one by Meyer-Peter and Müller, $q/V_s d = a(\theta - \theta_t)^{3/2}$, with dimensionless sand flux

$$Q = \left(\frac{|w|^2}{u_t^2} - 1 - \frac{1}{\mu}\,\partial_X H\right)^{3/2}. \tag{42}$$

Figure 8 shows that the corresponding dune profile is very similar to that given by the Fernandez Luque–van Beck law (see Fig. 6), with dune velocity smaller by 6% and volume smaller by about

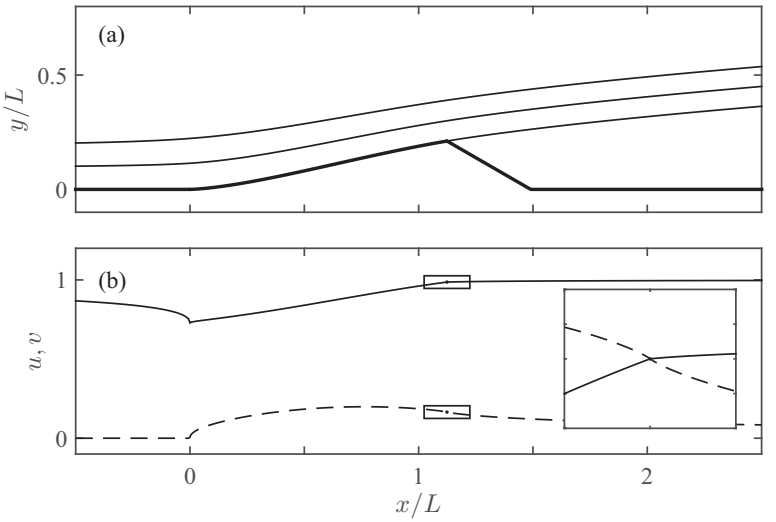

FIG. 7. Same as Figure 6, for the linearized sand transport law (41); the computed position of the separation point is $x_s = 1.12$ and the dune velocity and volume are $V = 25.2$ and $A = 0.148$ ($\mu = 0.5$, $u_t = 0.5$).

15%. It can be concluded that the dune characteristics are weakly dependent on the details of the sand transport equation.

IV. DISCUSSION

As mentioned in the introduction, a major feature of sand dunes is that they generally exhibit a sharp brink at which the flow separates, with an avalanche face on the lee side. The question of the determination of the separation point, and the need of a rational criterion for that, has been underestimated until today, or solved with *ad hoc* arguments such as an arbitrary "cut" of a smooth

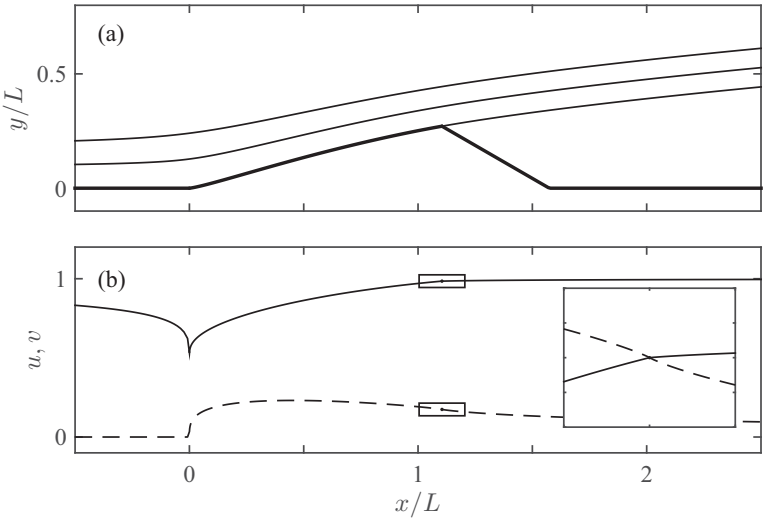

FIG. 8. Same as Fig. 6, for the Meyer-Peter and Müller law (42); the computed position of the separation point is $x_s = 1.10$ and the dune velocity and volume are $V = 15.9$ and $A = 0.221$ ($\mu = 0.5$, $u_t = 0.5$).

dune at an empirically fixed percentage of its length. The present study shows that the Brillouin-Villat condition provides a rational answer to the question. In particular, this condition provides, in addition to the position of the separation point, the velocity of traveling dunes. It must be stressed that within the present model, the bed shear stress, provided by a classical closure law, is in phase with the flow velocity, so that the flat bed is linearly stable. Thus, it is the separation which allows the existence of a self-preserving dune shape.

Let us now briefly show how this model may be assessed with experiments. As an example, consider the aquatic barchan dunes studied by Franklin and Charru [23]. Although these dunes are three-dimensional, they exhibit a vertical symmetry plane where the fluid flow and sand motion can be considered as two-dimensional. In this symmetry plane, the dune profiles are well fitted by the cosine shape

$$h = h_e \cos \frac{\pi (x - L_e)}{2L_e} \quad \text{for} \quad 0 < x < x_{se},$$

where x_{se} is the location of the separation point. The typical dune shown in their Fig. 8, with $h_e = 3.6$ mm, $L_e = 45$ mm, and $x_{se} = 41$ mm, has two-dimensional volume $A_e = 99.7\,\text{mm}^2$ which gives the required length scale $A_e^{1/2} = 10.0$ mm.

Let us now compute, for this dune, the position $X_{s,\text{dim}}$ of the separation point as predicted by the Brillouin-Villat criterion. For the sake of simplicity and generality, we use the exponential solution (32) of the simplified problem, with separation point (36) at the dimensional location

$$X_{s,\text{dim}} = 0.854\, q_1 \frac{A_e^{1/2}}{(0.280 q_1 + 0.286)^{1/2}}, \tag{43}$$

where q_1 involves the sand transport parameters μ (the friction coefficient) and u_t (the threshold velocity divided by the fluid velocity at infinity). Keeping in view the uncertainties about the sand transport law, we choose $q_1 = 7.94$ so that the slope of the exponential solution at the dune foot, q_1^{-1}, fits the measured slope $h'(0) = 0.126$ [for the sand transport equation (26) and $u_t^2 = 0.5$, this corresponds to the reasonable friction coefficient $\mu = 0.13$]. Then Eq. (43) gives $X_{s,\text{dim}} = 4.27 A_e^{1/2} = 42.7$ mm. This value appears to be close to the measured one, $x_{se} = 41$ mm. Note that the cosine and exponential profiles are, for these parameter values, nearly indistinguishable. The parabolic fit of the dune shape also proposed by Franklin and Charru [23] leads to similar results. It can be concluded that the Brillouin-Villat criterion, although based on inviscid flow calculations, is able to provide reasonable predictions of the position of the separation point.

For a traveling dune, a feedback mechanism can now be described to exist, which would restore the Brillouin-Villat position of the brink if this brink were moved to a different position by an external perturbation. Let us consider, as an illustration, the dune represented in Fig. 7, for which the Brillouin-Villat condition gives $x_s = 1.12$ for the position of the separation point; the solid curve in Fig. 9 shows the fluid velocity $|w|$ increasing along the dune and reaching the value $|w| = 1$ at the brink. Now assume that the brink is perturbed slightly upstream, to $x_s = 1.10$, say, and compute the corresponding flow. Then, as shown by the dot-dashed line in Fig. 9, the fluid velocity on the dune surface is increased: This overspeed induces more erosion, which smooths out and moves forward the brink itself. On the opposite, for a perturbation stretching the dune, to $x_s = 1.16$, say, the fluid velocity upstream the brink is smaller than unity (dashed line), which corresponds to less erosion and receding of the brink to the left. A feedback mechanism is thus in place, tending to stabilize the brink right at the Brillouin-Villat position.

The dunes considered in this paper are isolated. In reality, dunes often appear in the form of dune fields, with wake interactions leading to splitting or merging [24]. Such interactions cannot be captured by the present analysis, since, as noted previously, the "wake" of dead fluid involved in the Helmholtz-Kirchhoff theory extends to infinity downstream. An incoming flux from upstream, leading to slow dune growth, however, may be added to the analysis and is left for future work.

As a final point, it must be noted that the Brillouin-Villat criterion appears, for the separation point over smooth obstacles or at the brink of erodible dunes, as the counterpart of the

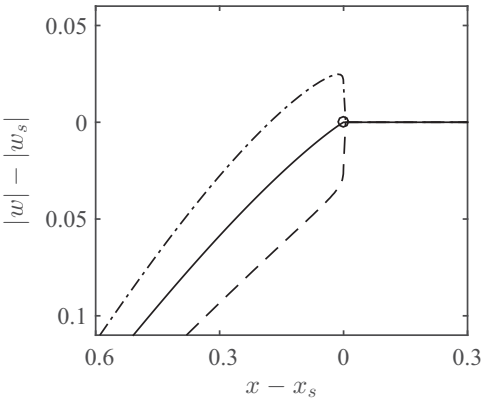

FIG. 9. Fluid velocity $|w|$ in the vicinity of the separation point, with the linearized sand transport law (41): (-.-), $x_s = 1.10$ imposed; (−), $x_s = 1.12$ satisfying the Brillouin-Villat condition; (- -), $x_s = 1.16$ imposed.

Kutta-Joukovsky condition for airfoils with sharp trailing edge. It determines, for a dune of given volume, a unique value of the dune velocity, just as the Kutta-Joukovsky condition determines a unique value of the circulation and the lift force on an airfoil.

[1] J. F. Kennedy, The mechanics of dunes and antidunes in erodible-bed channels, J. Fluid Mech. **16**, 521 (1963).

[2] F. Charru, B. Andreotti, and P. Claudin, Sand ripples and dunes, Ann. Rev. Fluid Mech. **45**, 469 (2013).

[3] A. Fourrière, P. Claudin, and B. Andreotti, Bedforms in a turbulent stream: Formation of ripples by primary linear instability and of dunes by non-linear pattern coarsening, J. Fluid Mech. **649**, 287 (2010).

[4] S. E. Coleman and B. W. Melville, Initiation of bed forms on a flat sand bed, J. Hydraul. Eng. **122**, 301 (1996).

[5] S. E. Coleman, J. J. Fedele, and M. H. Garcia, Closed-conduit bed-form initiation and development, J. Hydraul. Eng. **129**, 956 (2003).

[6] R. A. Bagnold, The flow of cohesionless grains in fluids, Phil. Trans. R. Soc., A **249**, 235 (1956).

[7] K. H. Andersen, A particle model of rolling grain ripples under waves, Phys. Fluids **13**, 58 (2001).

[8] G. Rousseaux, A. Stegner, and J. E. Wesfreid, Wavelength selection of rolling-grain ripples in the laboratory, Phys. Rev. E **69**, 031307 (2004).

[9] B. Andreotti, P. Claudin, and O. Pouliquen, Aeolian Sand Ripples: Experimental Study of Fully Developed States, Phys. Rev. Lett. **96**, 028001 (2006).

[10] B. Andreotti, P. Claudin, and S. Douady, Selection of dune shapes and velocities. Part 2: A two-dimensional modeling, Eur. Phys. J. B **28**, 341 (2002).

[11] K. Kroy, G. Sauermann, and H. J. Herrmann, Minimal model for aeolian sand dunes, Phys. Rev. E **66**, 031302 (2002).

[12] V. V. Sychev, V. V. Sychev, A. I. Ruban, and G. L. Korolev, *Asymptotic Theory of Separated Flows* (Cambridge University Press, Cambridge, UK, 1998).

[13] P.-Y. Lagrée, A triple deck model of ripple formation and evolution, Phys. Fluids **15**, 2355 (2003).

[14] G. K. Batchelor, *An Introduction to Fluid Dynamics* (Cambridge University Press, Cambridge, UK, 1967).

[15] T. Levi-Cività, Scie e leggi di resistenza, Rend. Circolo mat. di Palermo **23**, 1 (1907).

[16] M. Brillouin, Les surfaces de glissement d'Helmholtz et la résistance des fluides, Annal. Chimie Phys. **23**, 145 (1911).

[17] H. Villat, Sur la validité des solutions de certains problèmes d'hydrodynamique, J. Math. Pures Appl. **10**, 231 (1914).
[18] T. B. Benjamin, Shearing flow over a wavy boundary, J. Fluid Mech. **6**, 161 (1959).
[19] J. C. R. Hunt, S. Leibovich, and K. J. Richards, Turbulent shear flows over low hills, Q. J. R. Meteorol. Soc. **114**, 1435 (1988)
[20] P. Luchini and F. Charru, Quasilaminar regime in the linear response of a turbulent flow to wall waviness, Phys. Rev. Fluids **2**, 012601(R) (2017).
[21] E. Lajeunesse, L. Malverti, and F. Charru, Bedload transport in turbulent flow at the grain scale: Experiments and modeling, J. Geophys. Res. **115**, F04001 (2010).
[22] R. Fernandez Luque and R. van Beek, Erosion and transport of bed-load sediment, J. Hydraul. Res. **14**, 127 (1976).
[23] E. M. Franklin, and F. Charru, Subaqueous barchan dunes in turbulent shear flow. Part 1. Dune motion, J. Fluid Mech. **675**, 199 (2011).
[24] P. Hersen, K. H. Andersen, H. Elbelrhiti, B. Andreotti, P. Claudin, and S. Douady, Corridors of barchan dunes: Stability and size selection, Phys. Rev. E **69**, 011304 (2004).